HALDIA INSTITUTE OF TECHNOLOGY
Hatiberia, Haldia - 721657
West Bengal, India.
https://hithaldia.in

Dr. Gourisankar Roymahapatra
PhD (Science), FICS, FIC, FRESI
Associate Professor of Chemistry
Department of Applied Sciences & Humanities

Date: 26th June, 2023

Sub: Accepting your collaborative research proposal- Reg.

To,
Prof. Sibaprasad Maity
Principal,
Sagardighi Kamada Kinkar Smriti Mahavidyalaya,
Sagardighi, Murshidabad,
West Bengal 742226, India.

Dear Prof. Maity,

It is indeed a good assertion to carry out collaborative theoretical research with your good self. During your stay at **Haldia Institute of Technology** we together accomplished computational chemistry research with *Density Functional Theory (DFT)* which ultimately divulged into a Journal of repute in the field of *Chemosensor*.

As an upshot of my current field of interest, I am synthesizing some *Chitosan based hydrogel*, *Schiff base* metal complexes, designing *Hydrogen storage materials*, *N-Heterocyclic ligands and complexes*, including *computational chemistry based on DFT*.

Keeping in view of your significant contribution in the arena of organic synthesis, it will proliferate and fortify the motto of the group i am associated with. I strongly believe that this collaboration will strengthen our resources to achieve mutual goals and make a significant impact in chemistry research, and I hope this will be extremely beneficial for both the organizations; *Haldia Institute of Technology* and *Sagardighi Kamada Kinkar Smriti Mahavidyalaya;* in all aspects.

It is better if you can arrange a meeting (may be offline or online) to discuss the mutual objectives for further proceedings.

Extending my regards and thanks,

Dr. Gourisankar Roymahapatra
HIT Haldia

Dr. Gourisankar Roymahapatra
Associate Professor
Dept. of Applied Sciences
Haldia Institute of Technology
Haldia-721657.WB.

e-Mail: grm.chem@gmail.com; grm.chem@hithaldia.in
Mob:+91-9434452931 / +91-7001316547(WA)

Engineered Science

Hydrogen Storage Efficiency of Ag (I)/Au (I) Decorated Five-Member Aromatic Heterocyclic (AH) Compounds: A Theoretical Investigation

Abhishek Bag,[1,2] Swapan Sinha,[1] Himadri Sekhar Das,[1,3] Santanab Giri,[1] Gobinda Chandra De,[2] Sibaprasad Maity,[4] Ben Bin Xu,[5] Zhanhu Guo,[5] Jhuma Ganguly[6] and Gourisankar Roymahapatra[1,*]

Abstract

The hydrogen (H_2) economy has long faced significant challenges in the areas of production, storage, and application. Extensive research efforts have been directed towards finding effective solutions. Among the various storage options, solid-state hydrogen storage has emerged as a promising alternative. In this study, we conduct a theoretical investigation on the efficiency of H_2 trapping in Ag(I)/Au(I)-decorated five-member aromatic heterocyclic (AH) rings. We analyze the aromaticity of the metal-decorated ring and the H_2-trapped metal-decorated ring using the nuclear independent chemical shift (NICS) value, to study the stability of the aromatic system. Our findings also demonstrate that these systems are capable of trapping up to five molecules of H_2 in a quasi-sorption manner. Furthermore, we investigate the spontaneity of H_2 adsorption in Ag(I)/Au(I)-decorated systems by examining the Gibbs free energy change. To understand the bonding nature, we perform an analysis using the electron localization function (ELF) and non-covalent interaction (NCI) analysis, which reveal the bonding nature of our modeled systems. It has shown the gravimetric wt% values ranging from 3.66 to 5.45. Additionally, the partial density of states (PDOS) technique is employed to identify the contributions of H_2, decorated metal, and the five-member AH system towards the frontier molecular orbitals of the complexes. Also, ADMP calculation indicates their stability near room temperature.

1. Introduction

Hydrogen is increasingly recognized as the preferred energy carrier for the 21st century due to its clean, abundant, and non-toxic nature. When used as a fuel cell or burner, hydrogen produces only heat and water vapor, making it environment friendly. Therefore, the successful development of the hydrogen economy offers numerous advantages for the environment. However, a key challenge in advancing the hydrogen economy lies in the development of a safe, compact, lightweight, and cost-efficient hydrogen storage system. The widespread utilization of hydrogen as a fuel requires storage systems that offer high gravimetric weight percent (wt%) and volumetric density, rapid kinetics for ambient adsorption and desorption, favorable enthalpy for hydrogen adsorption and desorption, recyclability, safety, and cost-efficiency.[1,2] Therefore, designing structures based on reported systems and developing new systems to enhance H_2 trapping efficiency are popular research avenues. Due to the advantages of clean, renewable, abundant, and outstanding performance in terms of environment friendly, hydrogen has received much attention.[3-5] Safety and cost-effectiveness in hydrogen storage techniques are a big problem for hydrogen use in transportation applications.[6] Conventional storage methods

[1] *School of Applied Sciences and Humanities, Haldia Institute of Technology, ICARE Complex, Haldia 721657, WB, India.*

[2] *Department of Chemistry, Cooch Behar Panchanan Barma University, Cooch Behar 736101, WB, India.*

[3] *Department of ECE, Haldia Institute of Technology, ICARE Complex, Haldia 721657, WB, India.*

[4] *Department of Chemistry, Sagardighi Kamada Kinkar Smriti Mahavidyalaya, Sagardighi 742226, WB, India*

[5] *Mechanical and Construction Engineering, Faculty of Engineering and Environment, Northumbria University, Newcastle Upon Tyne NE1 8ST, UK.*

[6] *Department of Chemistry, Indian Institute of Engineering Science and Technology, Howrah 711103, WB, India.*

*Email: grm.chem@gmail.com (G. Roymahaptra)

such as pressurized hydrogen gas and liquid storage systems involve high safety and cost concerns for onboard applications.[7,8]

Therefore, alternative storage methods are highly obligatory to meet the necessities of the hydrogen economy. Solid-state storage systems based on metal hydrides, organometallic compounds, and metal clusters have shown great potential for storing hydrogen securely, compactly, and reversibly, making them an interesting area of research for hydrogen storage. However, none of these schemes fully satisfy all the essential criteria for a viable and sustainable hydrogen technology. Among all reported methods, solid-state hydrogen storage materials have attracted much attention,[9-12] such as hydride complexes,[13-16] polymeric material,[17-19] carbon nanomaterial,[20-23] and metal-organic frameworks (MOF).[24,25] Solid-state hydrogen storage materials have garnered significant interest due to their impending advantages. To be granted as efficient hydrogen storage materials, these systems should exhibit fast adsorption/desorption kinetics and high gravimetric density (5.5 wt%).[26] Hydrogen storage technology mainly divided into two types: physisorption process (the host materials adsorb H_2 molecules via weak interaction at very low temperatures and high hydrogen gas pressure) and chemisorption process (the H_2 molecule dissociates into atomic stage and then is bonded to the host materials). In both processes; during application; it is difficult to release H_2 molecule from the host due to strong interaction and hence it is difficult to use in transportation/automobile industries. Therefore, materials with reversible adsorption energy (0.2eV/H_2 to 0.6 eV/H_2) (4.612 kcal/mol to 13.836 kcal/mol)[27, 28] tend to meet high gravimetric density and release H_2 easily near room temperature. Metalized siligraphene nano-sheet (SiC$_7$) is a good example of such kind. It can operate as an efficient H_2 storage material at ambient conditions.[29] Light metal decorated C$_4$N nano-sheet can bind up to five H_2 molecules efficiently. Titanium and Boron decorated twin-graphene provides new inspiration for the discovery of carbon-based hydrogen storage materials.[30] Decoration of transition metal increases the hydrogen storage capacity at room temperature on different graphene sheets.[31] It is also found that alkali metal and transition metal decorated germanene are energetically favorable which serves as good hydrogen storage systems.[32] Transition metal doping also increases the hydrogen storage capacity of two-dimensional carbon-nitride nano-sheets.[33] Transition metal (TM= Sc, Ti, V, Cr, Mn) decorated covalent triazine-based framework shows potential hydrogen storage efficacy without cluster formation.[34] To be suitable for hydrogen storage, system must fulfill specific criteria: (a) H_2 adsorption occurs in the molecular state rather than atomic form, (b) cluster formation is avoided, (c) metals have a low weight, (d) they meet the targets set by the Department of Energy (DOE), and (e) adsorption occurs preferably through a quasi-adsorption process. In our group, we have recently reported many important findings regarding of Li-decorated aromatic heterocyclic systems,[35-41] which meets the target set by DOE (2025). It has also been found that clustering of Ti on a C60 surface show the high efficiency of hydrogen storage.[42] Very few works are reported on transition metal decorated heterocyclic systems because cluster formation (some of the results show that) will occur in metal complexes which lower the H_2 storage capacity. It is also reported that metal-metal clusters are very good materials for H_2 storage and in such cases material can avoid the metal aggregation problem. On the other hand; in most of the cases, the adsorption process is either physical adsorption or chemical adsorption. Through a comprehensive review of different hydrogen storage systems, it becomes apparent that metals exhibit excellent hydrogen adsorption and storage abilities. Very recently, one interesting report published in the J. Am. Chem. Soc. (2023), where scientists have synthesized and established air-stable Cu(I) metal-organic framework and it found to be excellent hydrogen storage[43] material, and it encouraged us to design and theoretically investigate the storage efficiency of various five-member aromatic heterocyclic rings decorated with coin metals, such as Ag and Au. In this paper objective is to explore their efficacy as hydrogen storage materials by analyzing their different properties and also to explore which system is more suitable for this purpose.

2. Theory and computational details

In this study, the designed systems were optimized to their local minimum on the potential energy surface with zero imaginary frequency using the Gaussian 16w quantum chemistry program package.[44] Density functional theory (DFT)[45] within different functional such as CAM-B3LYP, M05, and various basis sets including 6-311+g (d, p), 6-31+G*, and LanL2DZ were employed. Bare rings were optimized at CAM-B3LYP/6-311+g(d, p). On the other hand we have optimized with and without H_2 trapped metal decorated model systems taken two basis set 6-31+G* (for ring atoms) and LanL2DZ (for metal atom) with M05 function for DFT calculation.

The stability and chemical reactivity of the Ag(I)/Au(I)-AH systems and their H_2-trapped complexes were analyzed using conceptual DFT (CDFT)-based descriptors such as hardness (η) and electrophilicity (ω), calculated with standard techniques[46-48] Basically hardness and electrophilicity are the global property of model systems. Increasing value of hardness indicate the increasing stability of the systems. On the other hand decreasing value of electrophilicity indicates decreasing reactivity of the systems.

The average binding energy (E_b) value of each Ag(I)/Au(I)-AH systems are determined using Eq-(1)

$$E_b = [E_{(host)+@nH2} - (E_{(host)+} + nE_{H2})]/n \qquad (1)$$

Where $E_{(host)+@nH2}$, $E_{(host)+}$ and E_{H2} represent the energy of the gradual H_2 trapped Ag(I)/Au(I)decorated heterocyclic system, only Ag(I)/Au(I)decorated heterocyclic system and energy of H_2 molecule. 'n' symbolizes the number of H_2 molecule

trapped.

The average adsorption energy (Eads) of H_2 molecules is calculated using the Eq-(2)

$$E_{ads} = [(E_{(host)+} + nE_{H2}) - E_{[(host)+@nH2]}]/n \qquad (2)$$

Where $E_{(host)+@nH2}$, $E_{(host)+}$ and E_{H2} represent the energy of the gradual H_2 trapped Ag(I)/Au(I)decorated heterocyclic system, only the Ag(I)/Au(I)-decorated heterocyclic system and energy of H_2 molecule. 'n' symbolizes the number of H_2 molecule trapped.

We have also calculated nucleus independent chemical shift which is also called NICS. It is a very essential computational tools for the assessment of aromaticity. This method was invented by the late Paul V.R. Schleyer in the year 1996. Currently it is the most widely used method for determining and justifying aromaticity and antiaromaticity. At the time of calculation of NICS, a ghost atom, Bq is placed at the center of ring plane (denoted as NICS(0)) which is generally account for σ aomaticity and take another ghost atom Bq1 to 1Å above the center of the molecular plane(denoted as NICS(1)) which is denoted as π aromaticity. If the NICS(0) and NICS(1) value of a ring become negative then the systems are both σ and π aromatic in nature but if the value is positive then the systems becomes antiaromatic. We have calculated the NICS (0) and NICS(1) (nucleus independent chemical shift) values to check the pattern of aromaticity and stability of the metal decorated AH-systems as well as for Ag(I)/Au(I)-AH-systems.[49-51]

Gravimetric wt% was calculated to determine the hydrogen storage potential of the materials by the Eq-(3)

$$\text{Gravimetric wt\%} = \frac{Molecular\ weight\ of\ trapped\ H_2}{Molecular\ weight\ of\ (host) + @nH2} \times 100 \qquad (3)$$

To investigate the spontaneity of the hydrogen adsorption process, Gibbs free energy change with temperature was calculated using the following Eq- (4):

$$\Delta G_{(host@nH2)+} = [G_{(host@nH2)+} - G_{(host)+} - nG_{H2}] \qquad (4)$$

To analyze the bonding nature in the different systems, topological analysis was performed using the Multiwfn package.[52] The shaded surface map and electron localization function (ELF) were calculated to provide information about the localized electron.[53] Non-covalent interaction (NCI) analysis was conducted to identify non-covalent interactions in the Ag(I)/Au(I)-AH@nH$_2$ systems. The NCI results were generated using the Multiwfn software package.[54] Atom centered density matrix propagation (ADMP)[55-57] study has been carried out to know about the kinetic stability of model systems. Partial Density of States (PDOS) can be generated for different parts of the H_2-trapped metal-decorated complexes to identify the contribution of trapped H_2, decorated metal, and aromatic heterocyclic ring to the frontier molecular orbitals of the complexes.[58]

3. Result and discussion
3.1 Stability, and reactivity of different five-member heterocyclic systems

The study investigated the ground state geometry of various five-member AH systems, including imidazole, pyrazole, isoxazole, isothiazole, thiazole, and oxazole (Fig. 1). From the
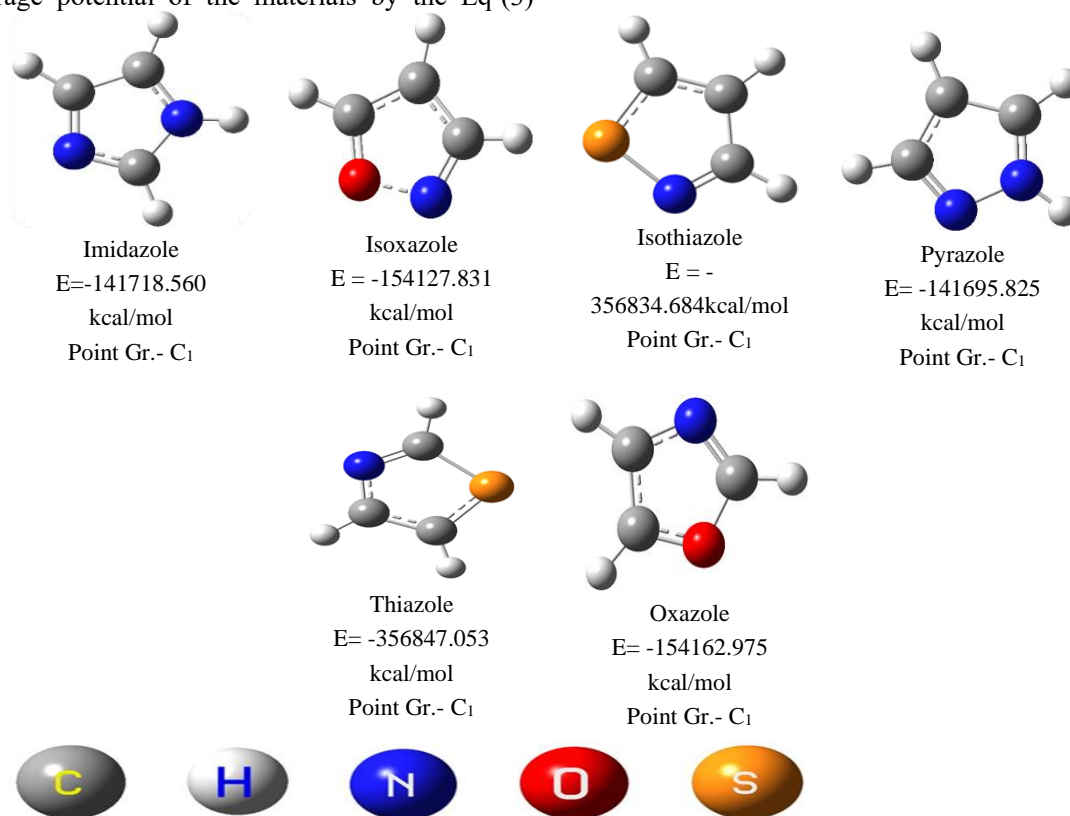

Imidazole
E=-141718.560 kcal/mol
Point Gr.- C$_1$

Isoxazole
E = -154127.831 kcal/mol
Point Gr.- C$_1$

Isothiazole
E = -356834.684kcal/mol
Point Gr.- C$_1$

Pyrazole
E= -141695.825 kcal/mol
Point Gr.- C$_1$

Thiazole
E= -356847.053 kcal/mol
Point Gr.- C$_1$

Oxazole
E= -154162.975 kcal/mol
Point Gr.- C$_1$

Fig. 1 Optimized geometries and energy of five-member AH-systems at the CAM-B3LYP/6-311+g (d,p) level of theory.

Table 1. Hardness (η);(kcal/mol), Electrophilicity (ω);(kcal/mol) and NICS(0) and NICS (1) of different five-member AH-systems. Hardness/atom & Electrophilicity/atom are in brackets.

Heterocyclic System	η (kcal/mol)	ω (kcal/mol)	NICS(0) (ppm)	NICS(1) (ppm)
Imidazole	225.593(25.065)	130.763(14.529)	-12.679	-10.475
Isoxazole	228.063(28.507)	167.646(20.955)	-11.924	-10.503
Isothiazole	221.837(27.729)	151.734(18.966)	-12.883	-11.093
Pyrazole	238.209(26.467)	132.364(14.707)	-13.279	-11.249
Thiazole	199.469(24.933)	167.185(20.898)	-12.417	-10.983
Oxazole	236.365(29.545)	151.273(18.909)	-11.063	-9.617

DFT calculation It was found that pyrazole exhibited the highest hardness value. As the hardness indicate the stability of the system so pyrazole is the most stable system, while isoxazole had a high electrophilicity value, suggesting it as the most reactive among the investigated systems (Table 1). All of the AH systems displayed negative NICS (0) and NICS (1) values, confirming their aromatic nature.

3.2 Stability, reactivity, aromaticity, and NBO of Ag(I)/Au(I) decorated differently studied five-membered aromatic heterocyclic systems

Metal-decorated systems [Ag(I)/Au(I)-AH] were created for H_2 adsorption by placing metal ions (Ag(I)/Au(I)) on the side and top of the five-member heterocyclic ring. After optimization, it was observed that the metal ions were predominantly bonded with the ring through the nitrogen (N) center. In case of oxazole, Ag(I)/Au(I) attached to both nitrogen (N) and oxygen (O) centers (Fig. 2), but the N-Ag(I)/Au(I) bonding was found to be the more stable isomer. Similarly, for isoxazole, isothiazole, and thiazole, Ag(I)/Au(I) primarily attached to the ring through the N atom rather than other ring electronegative atoms (O, S). The optimized structures of the metal decorated AH systems are provided in Fig. 2.

To assess the stability of the metal-decorated AH systems, various CDFT parameters such as hardness (η), electrophilicity (ω), NICS (0), NICS (1), and NBO (natural bond orbital) values were calculated (Table 2). The metal-decorated isoxazole system exhibited the highest hardness value, indicating greater stability, while Ag(I)-isoxazole system indicate higher hardness value than Au(I)-isoxazole system. The Ag(I)/Au(I)-decorated oxazole-O systems has shown higher electrophilicity, suggesting higher reactivity of the systems. On the basis of hardness value of all the Ag(I)/Au(I) decorated system, Ag(I)-decorated systems give higher stability (hardness range:73.317kcal/mol to 114.902 kcal/mol) than Au(I) decorated systems (hardness range: 54.298 kcal/mol to 103.883 kcal/mol). The negative NICS(0) and NICS(1) values confirmed aromatic nature of the investigated systems. Additionally, positive NBO charges on Ag or Au indicated the presence of an electric field, suggesting preferential H_2 adsorption on a metal site, enabling greater adsorption of up to five H_2 molecules. From Table 2, it is also

Table 2. Hardness (η);(kcal/mol), Electrophilicity (ω);(kcal/mol), NICS (0) and NICS (1) (ppm) and NBO charges on metal center of Ag^+/Au^+-decorated systems. Hardness/atom and Electrophilicity/atom values are in brackets.

System decorated with Ag+/Au+	η (kcal/mol)	ω (kcal/mol)	NICS(0) (ppm)	NICS(1) (ppm)	NBO
Imidazole-Ag⁺	106.688 (10.669)	207.877 (20.788)	-13.063	-11.149	0.909
Isoxazole-Ag⁺	114.902 (12.767)	225.203 (25.023)	-11.753	-10.984	0.931
Isothiazole-Ag⁺	105.609 (11.734)	232.722 (25.858)	-12.230	-11.798	0.924
Pyrazole-Ag⁺	101.932 (10.193)	237.027 (23.703)	-13.161	-11.868	0.911
Thiazole-Ag⁺	101.561 (11.285)	235.635 (26.182)	-12.228	-11.826	0.909
Oxazole-O-Ag⁺	73.317 (8.146)	362.944 (40.327)	-11.197	-9.748	0.963
Oxazole-N-Ag⁺	103.425 (11.492)	239.604 (26.603)	-11.918	-10.458	0.925
Imidazole-Au⁺	89.840 (8.984)	285.206 (28.521)	-12.937	-11.296	0.787
Isoxazole-Au⁺	103.883 (11.543)	285.672 (31.741)	-11.728	-10.899	0.831
Isothiazole-Au⁺	97.025 (10.781)	289.140 (32.127)	-12.051	-11.580	0.813
Pyrazole-Au⁺	93.454 (9.345)	296.042 (29.604)	-13.077	-11.696	0.793
Thiazole-Au⁺	94.778 (10.531)	289.366 (32.152)	-12.224	-11.725	0.788

Oxazole-O-Au$^+$	54.298(6.033)	577.005 (64.112)	-11.296	-9.616	0.897
Oxazole-N-Au$^+$	95.487(10.610)	299.025 (33.225)	-11.850	-10.359	0.815

observed that, the grater NBO charges on Ag(I) rather than Au(I), indicates grater adsorption of H$_2$-molecule on Ag(I)decorated systems.

3.3 Stability, reactivity, aromaticity, and NBO charges of highest no. of H$_2$ trapped Ag(I)/Au(I)- decorated different five-membered aromatic heterocyclic systems

The study examined the H$_2$ trapping capacity of the metal-decorated AH systems, revealing that all systems could trap a maximum of five H$_2$ molecules. All the optimized structures of the maximum H$_2$ trapped system [Ag(I)/Au(I)-AH@5H$_2$] have been given in Fig. 3 and consequently other lower no. H$_2$ trapped systems (1-4) have been shown in Fig. S1.
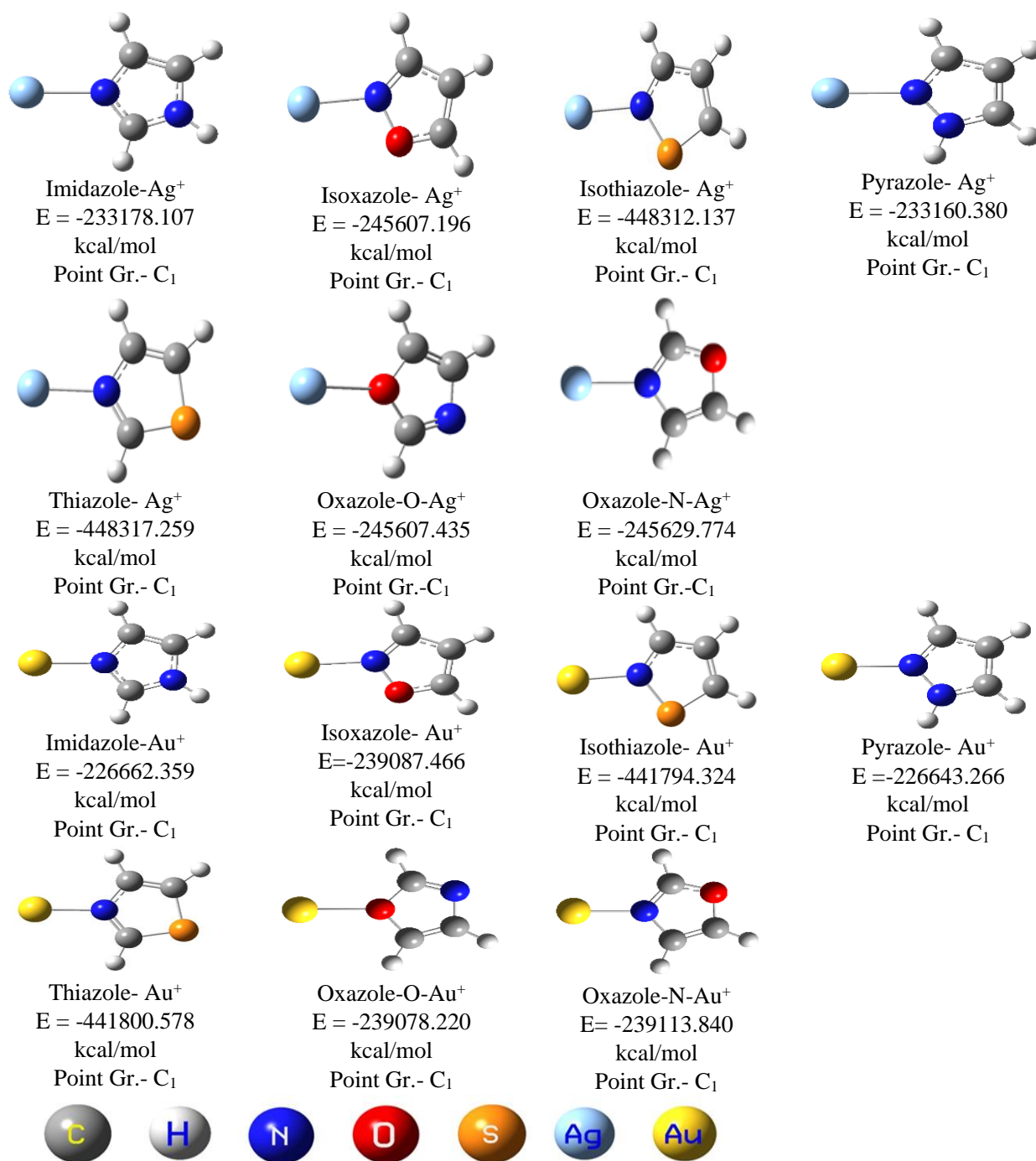

Fig. 2 Optimized geometries and energy of Ag$^+$ and Au$^+$ decorated different five-membered AH systems at the M05/ LanL2DZ (for Ag$^+$ and Au$^+$) and 6-31+G* (for ring atom) level of theory.
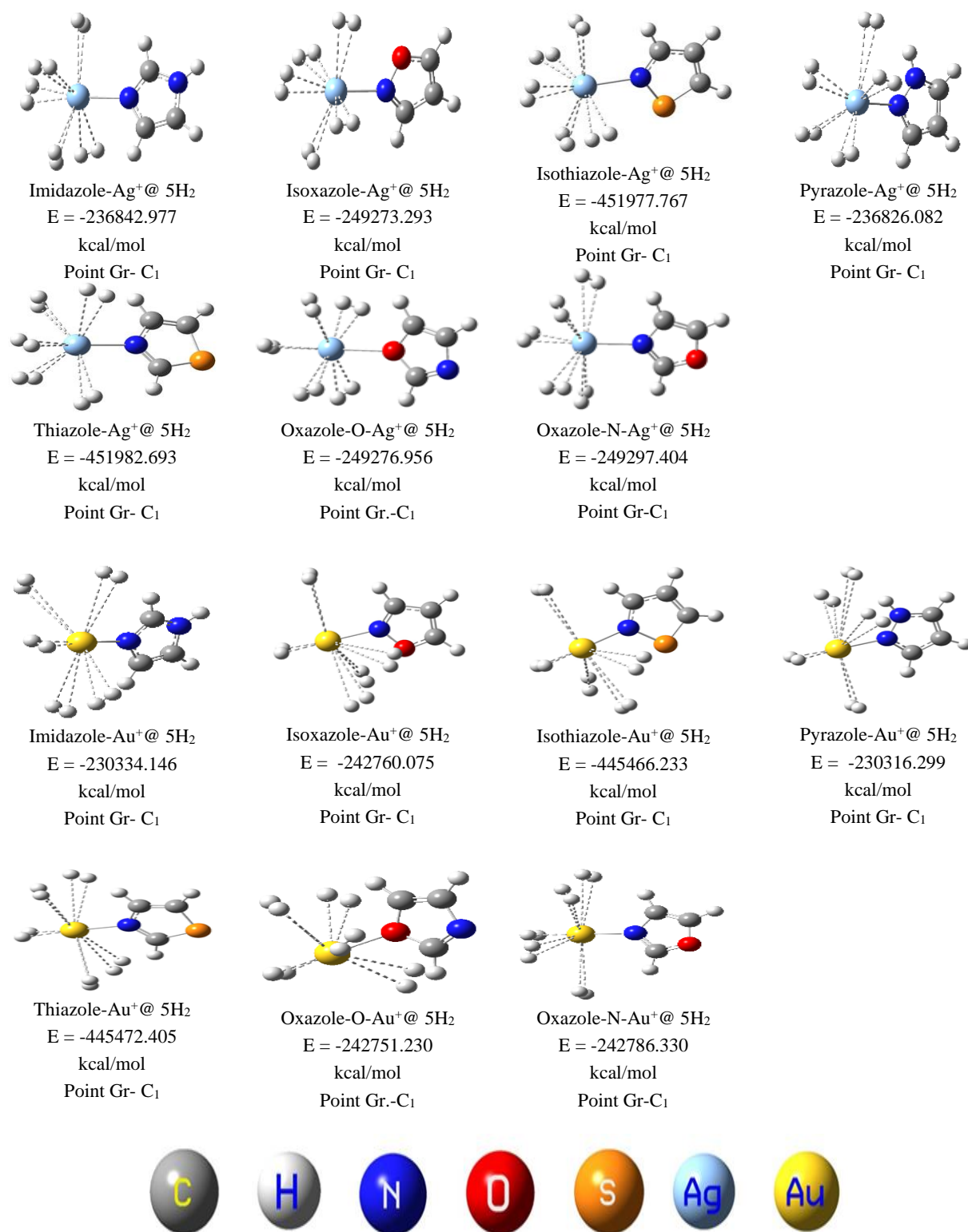
Imidazole-Ag$^+$@ 5H$_2$
E = -236842.977
kcal/mol
Point Gr- C$_1$

Isoxazole-Ag$^+$@ 5H$_2$
E = -249273.293
kcal/mol
Point Gr- C$_1$

Isothiazole-Ag$^+$@ 5H$_2$
E = -451977.767
kcal/mol
Point Gr- C$_1$

Pyrazole-Ag$^+$@ 5H$_2$
E = -236826.082
kcal/mol
Point Gr- C$_1$

Thiazole-Ag$^+$@ 5H$_2$
E = -451982.693
kcal/mol
Point Gr- C$_1$

Oxazole-O-Ag$^+$@ 5H$_2$
E = -249276.956
kcal/mol
Point Gr.-C$_1$

Oxazole-N-Ag$^+$@ 5H$_2$
E = -249297.404
kcal/mol
Point Gr-C$_1$

Imidazole-Au$^+$@ 5H$_2$
E = -230334.146
kcal/mol
Point Gr- C$_1$

Isoxazole-Au$^+$@ 5H$_2$
E = -242760.075
kcal/mol
Point Gr- C$_1$

Isothiazole-Au$^+$@ 5H$_2$
E = -445466.233
kcal/mol
Point Gr- C$_1$

Pyrazole-Au$^+$@ 5H$_2$
E = -230316.299
kcal/mol
Point Gr- C$_1$

Thiazole-Au$^+$@ 5H$_2$
E = -445472.405
kcal/mol
Point Gr- C$_1$

Oxazole-O-Au$^+$@ 5H$_2$
E = -242751.230
kcal/mol
Point Gr.-C$_1$

Oxazole-N-Au$^+$@ 5H$_2$
E = -242786.330
kcal/mol
Point Gr-C$_1$

Fig. 3 Optimized geometries and energy of highest no. of H$_2$ trapped Ag$^+$and Au$^+$-AH systems at the M05/ LanL2DZ (for Ag$^+$ and Au$^+$) and 6-31+G* (for ring atom) level of theory.

From Table 3, It is interestingly observed that Isoxazole-Ag+@5H$_2$ has the higher hardness value among other Ag(I) decorated system. Also it has observed that Isoxazole-Au$^+$@5H$_2$ system has the higher hardness value among other Au(I) decorated system. So, among Ag(I)-decorated system, Isoxazole-Ag$^+$@5H$_2$ system is the most sable systems. In other side, among Au(I)decorated system, Isoxazole-Au$^+$@5H$_2$ is most stable one. Between H$_2$ trapped Ag(I) and Au(I)decorated system, Au(I)-decorated systems exhibit higher stability (hardness range: 105.784 kcal/mol to 162.536 kcal/mol) than Ag(I)-decorated system (hardness range: 113.076 kcal/mol to 152.433 kcal/mol). If we have observed

Table 3. Hardness (η);(kcal/mol), Electrophilicity (ω);(kcal/mol), NICS(0) and NICS (1) and NBO charges on metal center of highest no. of H$_2$ trapped Ag$^+$/Au$^+$-AH systems. Hardness/atom & Electrophilicity/atom are in brackets.

System decorated with M$^+$	η(kcal/mol)	ω(kcal/mol)	NICS(0) (ppm)	NICS(1) (ppm)	NBO
Imidazole-Ag$^+$@5H$_2$	133.514(6.676)	130.262(6.513)	-12.964	-11.690	0.764
Isoxazole-Ag$^+$@5H$_2$	152.433(8.023)	133.942(7.050)	-11.623	-11.008	0.753
Isothiazole-Ag$^+$@5H$_2$	141.860(7.466)	137.670(7.246)	-12.115	-12.056	0.807
Pyrazole-Ag$^+$@5H$_2$	138.176(6.909)	138.301(6.915)	-13.036	-12.701	0.760
Thiazole-Ag$^+$@5H$_2$	138.076(7.267)	137.080(7.215)	-12.127	-12.011	0.762
Oxazole-O-Ag$^+$@5H$_2$	113.076(5.951)	181.032(9.528)	-11.248	-9.918	0.773
Oxazole-N-Ag$^+$@5H$_2$	140.448(7.392)	139.368(7.335)	-11.835	-10.540	0.768
Imidazole-Au$^+$@5H$_2$	147.758(7.388)	125.382(6.269)	-12.889	-12.070	0.629
Isoxazole-Au$^+$@5H$_2$	162.536(8.555)	136.466(7.182)	-15.859	-13.515	0.656
Isothiazole-Au$^+$@5H$_2$	147.670(7.772)	145.124(7.638)	-11.933	-11.618	0.638
Pyrazole-Au$^+$@5H$_2$	151.824(7.591)	133.308(6.665)	-13.016	-11.800	0.634
Thiazole-Au$^+$@5H$_2$	148.806(7.832)	137.061(7.214)	-12.089	-11.577	0.634
Oxazole-O-Au$^+$@5H$_2$	105.784(5.568)	228.668(12.035)	-11.525	-14.717	0.724
Oxazole-N-Au$^+$@5H$_2$	153.550(8.082)	136.726(7.196)	-11.808	-10.525	0.643

the electrophilicity value of the different H$_2$ trapped metal decorated systems, then we have noticed that H$_2$ trapped Au(I) decorated imidazole system has become less reactive among other Au(I) decorated systems. On the other hand H$_2$ trapped Ag(I) decorated Imidazole system has shown less reactivity among other Ag(I) decorated systems. Between Ag(I) and Au(I) decorated systems, Ag(I) decorated model systems show the better results (electrophilicity range:130.262kcal/mol to181.032 kcal/mol) than Au(I) decorated model systems (electrophilicity range:125.382 kcal/mol to 228.668 kcal/mol).The hardness and electrophilicity values generally increased and decreased, respectively, as the number of trapped H$_2$ molecules increased, indicating chemical stability.[59,60] Fig. S2 shows the graphical representation of hardness and electrophilicity values with gradual trapping of H$_2$ molecules of Ag(I)/Au(I)-AH systems. The hardness & electrophilicity value of different studied systems with gradual trapping of H$_2$ has been shown in Table S1. From Table 3, it is also observed that, at H$_2$-trapping condition, all the metal decorated AH- systems show negative NICS value, indicating their good aromatic nature. The

adsorption capacity was evaluated through the average adsorption energy (E$_{ads}$), which decreased with the gradual addition of H$_2$ molecules due to steric hindrance (Fig. 4). The value of average adsorption energy for all the H$_2$ trapped complexes are in between 0.11 eV/H$_2$ to 0.69 eV/H$_2$ (2.536 kcal/mol to 15.911 kcal/mol), which is intermediate of physisorption and chemisorption state. Thermodynamically, the adsorption process is spontaneous. The studied systems exhibited negative NICS(0) and NICS(1) values, indicating their good σ and π aromatic nature.

It is also observed that the energy of systems decreases at different stages like bare ring, metal (Ag (I)/Au (I)) decorated ring and H$_2$-trapped metal (Ag (I)/Au (I)) decorated ring. From Table 4 and 5, it has shown that the energy become decreases from bare ring to metal decorated systems and lastly it comes to the lower value in case of H$_2$ trapped metal decorated system. This study has indicated the stability of our modeled systems.

We have also studied the NBO charge calculation on metal center with gradual trapping of H$_2$ molecules. This study has graphically represented in Fig. 5. When we go through without
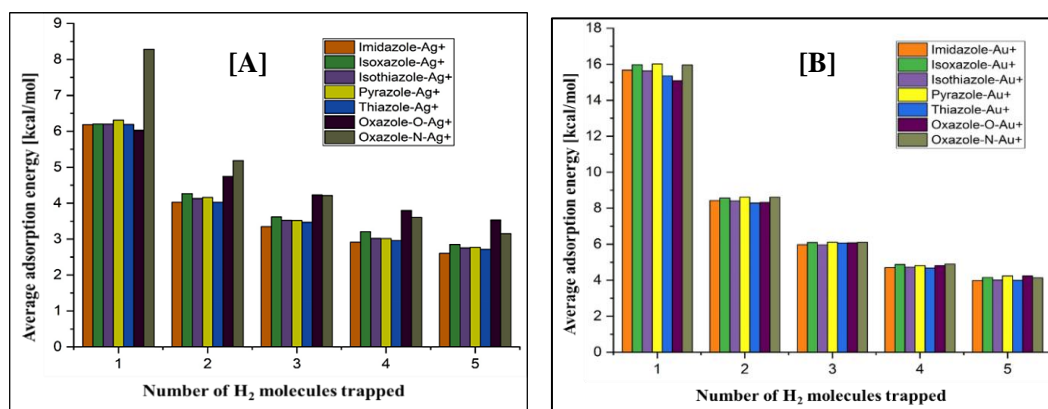

Fig. 4 A plot of Average adsorption energy [kcal/mol] Vs. no. of H$_2$ molecules trapped with Ag$^+$[A]and Au$^+$[B]-decorated different five-membered aromatic heterocyclic systems.

Table 4. Energy of the different systems at different stages like bare ring, metal [Ag(I)] decorated ring and H$_2$- trapped metal [Ag(I)] decorated ring at optimized condition.

Systems	Energy (kcal/mol)		
	Bare ring(kcal/mol)	Metal (Ag) decorated ring(kcal/mol)	H$_2$ trapped metal (Ag) decorated ring (kcal/mol)
Imidazole	-141718.560	-233178.107	-236842.977
Isoxazole	-154127.831	-245607.196	-249273.293
Isothiazole	-356834.684	-448312.137	-451977.767
Pyrazole	-141695.825	-233160.38	-236826.082
Thiazole	-356847.053	-448317.259	-451982.693
Oxazole-O	-154162.975	-245607.435	-249276.956
Oxazole-N	-154162.975	-245629.774	-249297.404

Table 5. Energy of the different systems at different stages like bare ring, metal [Au(I)] decorated ring and H$_2$- trapped metal [Au(I)] decorated ring at optimized condition.

Systems	Energy (kcal/mol)		
	Bare ring (kcal/mol)	metal (Au) decorated ring (kcal/mol)	H$_2$ trapped metal (Au) decorated ring (kcal/mol)
Imidazole	-141718.560	-226662.359	-230334.146
Isoxazole	-154127.831	-239087.466	-242760.075
Isothiazole	-356834.684	-441794.324	-445466.233
Pyrazole	-141695.825	-226643.266	-230316.299
Thiazole	-356847.053	-441800.578	-445472.405
Oxazole-O	-154162.975	-239078.221	-242751.230
Oxazole-N	-154162.975	-239113.840	-242786.330

H$_2$trapped and with H$_2$-trapped system, the NBO charges on the metal center decreases (from Table 2 to 3) which clearly indicate that H$_2$ adsorption takes places at the metal center. The gravimetric weight percentages of the H$_2$-trapped metal-decorated AH systems ranged from 3.66 to 5.45 for the highest number of trapped H$_2$ molecules (Table S2). Although these
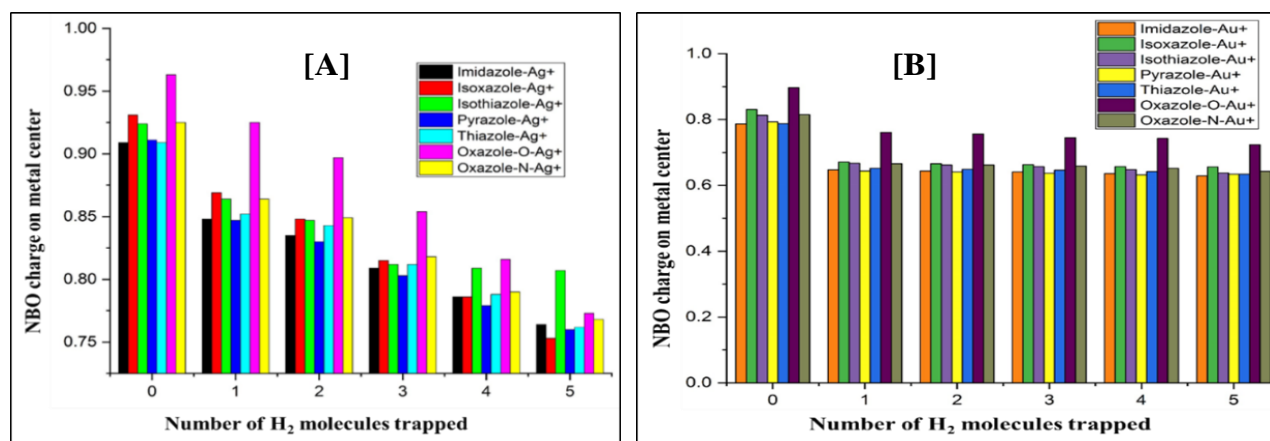
values were considered moderate compared to the U.S. Department of Energy (DOE) goal, the studied systems were still considered promising for H$_2$ storage. Among all the investigated systems, imidazole and pyrazole exhibited better results. The graphical representation of gravimetric wt% of maximum H$_2$ trapped Ag(I)/Au(I)-AH systems have been shown in Fig. S3.

3.4 Binding nature
3.4.1 Adsorption of hydrogen in molecular form
Table S4 shows that the Ag(I)/Au(I) to H$_2$ molecule distances in all the maximum H$_2$ trapped systems fall within the favorable range of 1.895 Å to 3.944 Å, which is suitable for a H$_2$ storage system. The H-H distances in all the trapped H$_2$ molecules range from 0.801 Å to 0.741 Å, similar to the distance in isolated H$_2$ molecules (0.743 Å).[61] Details of other systems can be found in Table S3.

3.4.2 Electron localization function (ELF)
To understand the binding nature between the ring and metal as well as metal and H$_2$ molecules, a detailed investigation was conducted using shaded surface maps and electron localization function (ELF) of the H$_2$ trapped Ag(I)/Au(I)-decorated systems. Fig. S4, S5, S6, and S7 display the shaded surface maps and ELF of H$_2$ trapped metal decorated studied systems. From ELF study in Fig. 6, it is clearly established that a non-covalent type interaction occurred between ring nitrogen (N) and metal center, as well as between metal center and molecular H$_2$ because between metal to ring and ring to molecular H$_2$, there is approximately zero electron density.

3.4.3 Non-covalent interaction (NCI)
The non-covalent interaction (NCI) method, also known as the reduced density gradient (RDG) method, is widely used for the analysis of weak interactions. NCI analysis plays a crucial role in identifying different types of interactions. In the NCI plot, the reduced density gradient (RDG) and the sign $(\lambda_2)\rho$ are plotted to represent the precise areas of interaction. The sign $(\lambda_2)\rho$ is used to differentiate between strong and weak non-

Fig. 5 A plot of NBO charge on metal center Vs. no. of H$_2$ molecules trapped with Ag$^+$ [A]and Au$^+$[B]-decorated different five-membered aromatic heterocyclic systems.
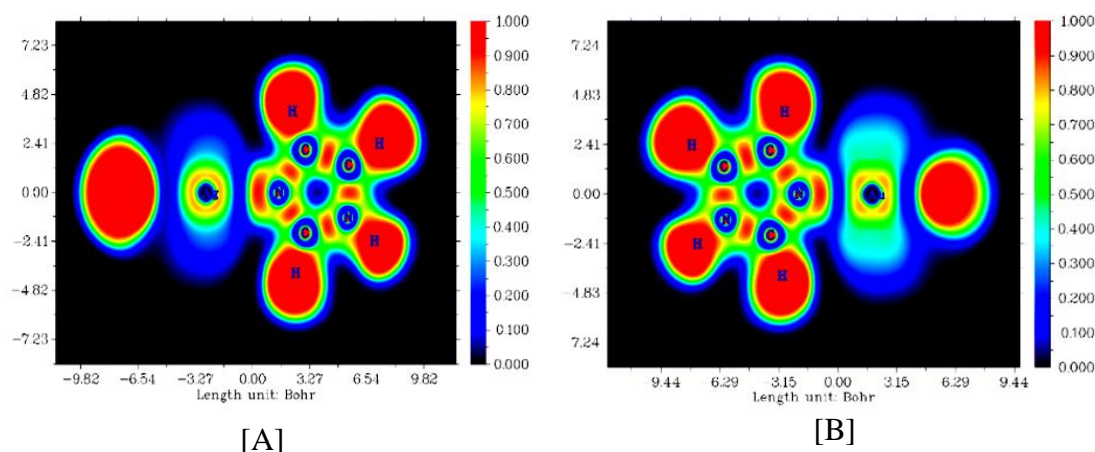
Fig. 6 The plot of the ELF of the H_2 trapped Ag(I)[A]/Au(I)[B] decorated Imidazole systems.

covalent interactions. In the NCI plot, the sign $(\lambda_2)\rho$ is placed on the X-axis, while the RDGs are displayed on the Y-axis. By using the Multiwfn software package, an interaction chart can be generated (Fig. 7) to visualize the areas in the NCI plot, where weak interactions occur.

The NCI plot of the Imidazole-Ag(I) system have been generated. It is observed that spikes appear in the zone where sign $(\lambda_2)\rho$ is approximately equal to 0 after the adsorption of the H_2 molecule (Fig. 8[B]). However, in the system without H_2 molecule trapping, no spikes are observed in the sign $(\lambda_2)\rho$ ≈ 0 zone in the NCI plot (Fig. 8[A]), which is clearly explain by the color chart(Fig. 7) This indicates the presence of weak interactions between the metal and molecular H_2, which satisfy the weak adsorption between them and favors the quasi-sorption process. The NCI plot of the other studied systems is shown in Fig. S8.

3.4.4 Partial density of state (PDOS)
To obtain a detailed analysis of the contribution pattern of the hydrogen molecule, metal ion, and the different aromatic heterocyclic rings towards the formation of frontier molecular orbitals (FMOs), we performed density of state (DOS) and partial density of state (PDOS) calculations for all the studied systems, as shown in Fig. 9.

Figure 9 presents the DOS and PDOS of the hydrogen-trapped Imidazole-Ag(I)/Au(I)-AH systems, indicating the

percentage contribution of H, metal ion, and aromatic heterocyclic systems towards the frontier molecular orbitals (FMOs). We divided the entire system into three different parts: trapped H_2, metal ion, and aromatic heterocyclic ring, and analyzed their respective contributions to the FMOs. From the DOS and PDOS values of the different systems, it can be concluded that all the fragments of the different systems significantly contribute to the formation of the frontier molecular orbitals (FMOs). The HOMO (highest occupied molecular orbital) and LUMO (lowest unoccupied molecular orbital) of the complexes are formed from the contributions of the aromatic heterocyclic ring, metal ion, and trapped molecular hydrogen, respectively.[62,63] The PDOS plots for other systems can be found in the supporting information, Fig. S9.

3.5 Effect of temperature on H_2 adsorption
To investigate the spontaneity of the reversible hydrogen adsorption-desorption process, we calculated the gibbs free energy change (ΔG) for the Imidazole system (with the highest gravimetric wt%). The results are shown in Fig. 10. It is found that at 298K, some systems exhibit a negative value of gibbs free energy, and we have wanted to investigate the specific temperature at which all the systems show a negative ΔG value.
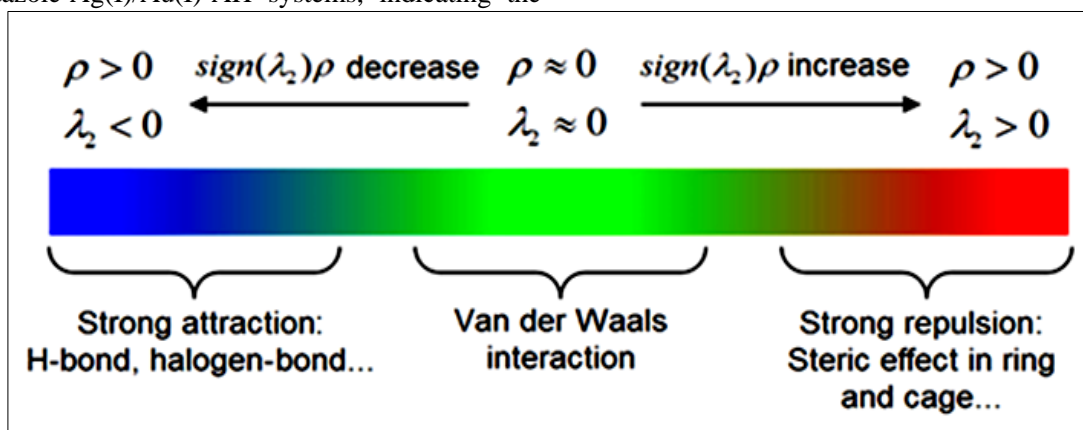

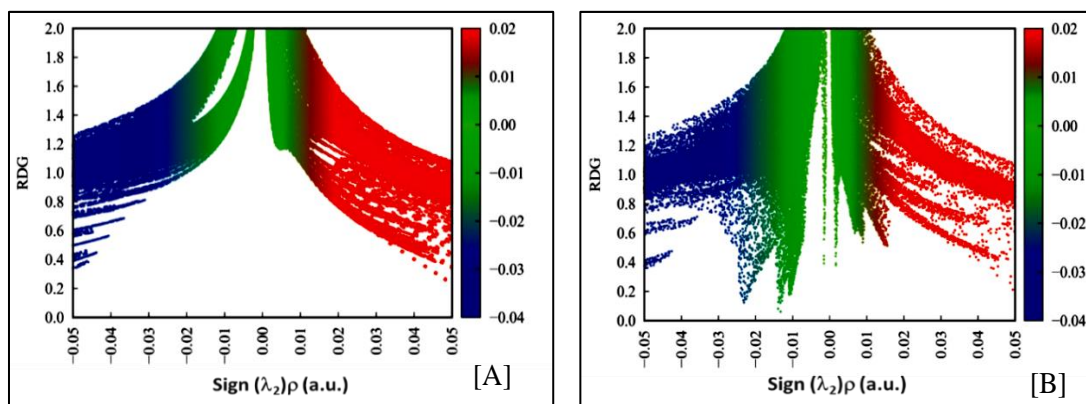**Fig. 7** Chart for viewing different interaction zone correspond to sign $(\lambda_2)\rho$ value in NCI plot.

Fig. 8 NCI plot of Imidazole-Ag⁺system without trapping of molecular H₂[A] and trapped with molecular H₂ [B].
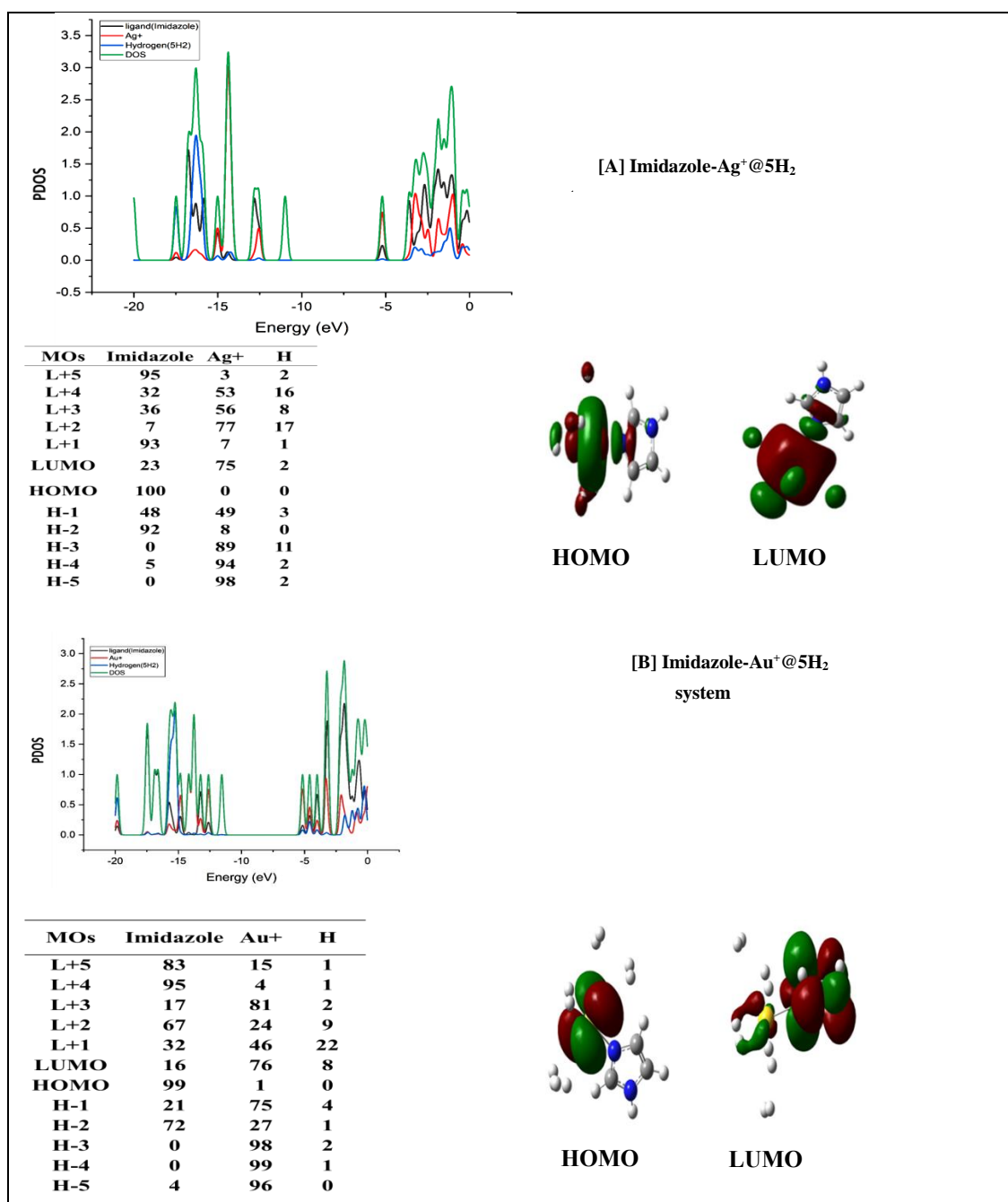

MOs	Imidazole	Ag+	H
L+5	95	3	2
L+4	32	53	16
L+3	36	56	8
L+2	7	77	17
L+1	93	7	1
LUMO	23	75	2
HOMO	100	0	0
H-1	48	49	3
H-2	92	8	0
H-3	0	89	11
H-4	5	94	2
H-5	0	98	2

MOs	Imidazole	Au+	H
L+5	83	15	1
L+4	95	4	1
L+3	17	81	2
L+2	67	24	9
L+1	32	46	22
LUMO	16	76	8
HOMO	99	1	0
H-1	21	75	4
H-2	72	27	1
H-3	0	98	2
H-4	0	99	1
H-5	4	96	0

Fig. 9 DOS & PDOS of hydrogen trapped [A] Imidazole-Ag⁺-AH and [B] Imidazole-Au⁺-AH systems with % of contribution of trapped H₂, metal ion & aromatic heterocyclic systems towards FMOs with their HOMO & LUMO picture.
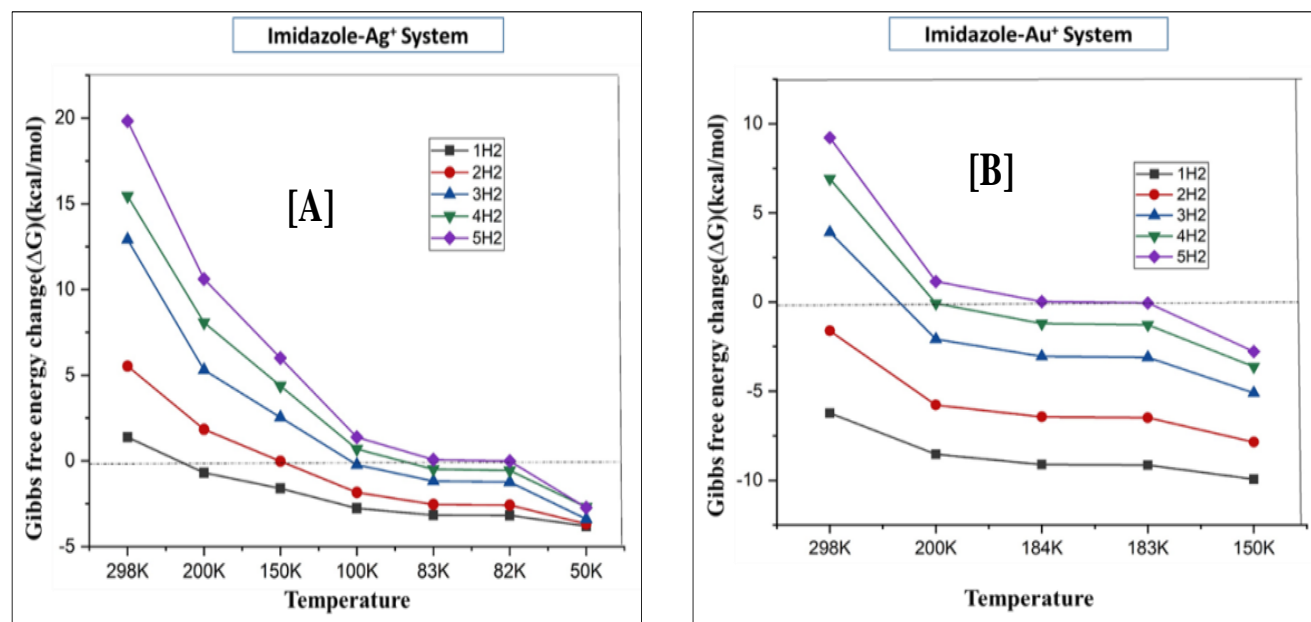
Fig. 10 Gibbs free energy change (kcal/mol) Vs. the number of H$_2$ molecules trapped with the Ag$^+$/Au$^+$-decorated Imidazole systems at different temperature.

Therefore, we decreased the temperature from 298K to 200K and later to 150K. As we considered different AH systems decorated with Ag(I)/Au(I), an investigation has performed to identify the the temperature at which a particular system exhibits a negative ΔG value. It was observed that at 82K and 183K, the Imidazole-Ag(I)@5H$_2$ and Imidazole-Au(I)@5H$_2$ systems, respectively, displayed a negative value of gibbs free energy (Fig. 10). All the systems decorated with Au(I) show the higher temperature for negative ΔG value but on the other hand Ag(I)decorated systems show very lower temperature for this purpose. The results for other systems are shown in Fig. S10, and Table S5. This study has indicated that Au(I) decorated systems show the batter temperature than Ag(I)-decorated systems for reversible hydrogen adsorption-desorption process.

3.6 Atom centered density matrix propagation (ADMP) study

As we all know that Ag(I) compounds are easily reduced in H$_2$ occlusion, so we want to investigate the condition of Ag(I)-decorated model system upon H$_2$ adsorption. Due to this reason, atom centered density matrix propagation (ADMP) study has been carried out at two different temperatures (200 K & 300 K) to investigate the kinetic stability of the Ag(I)/Au(I)AH@nH$_2$ systems (AH = Imidazole) (n=2). Here we have selected imidazole complex due to highest gravimetric wt % among others. As a consequence, we used a 1 fs time interval and a velocity scaling thermostat to keep the temperature constant throughout the simulation. The graphs of potential energy (E, A.U.) vs. time (t, fs) have been given in Fig. 11. From Fig. 11, it is clear that; complexes can retain H2 molecules at lower temperature up to 1000 fs. But the desorption starts when the temperature is increased. Lastly at room temperature at least one molecular H2 is attached to the

systems. From this it can be concluded that both metal decorated model systems survive upon H2 adsorption even at room temperature.

4. Conclusion

In this study, the hydrogen storage capacity of different heterocyclic aromatic systems (Imidazole, Isoxazole, Isothiazole, Pyrazole, Thiazole & Oxazole) decorated with Ag(I)/Au(I) were analyzed. The NICS values confirmed the aromatic nature of the studied systems prevail after the metal binding with AH and even after the hydrogen adsorption on the metal-AH system. The CDFT parameters provided insights into the stability and reactivity of the systems. The decreasing trends of the average adsorption energy and NBO charge on the Ag(I)/Au(I) site further supported the process of hydrogen adsorption. The negative Gibbs free energy change (ΔG) indicated the spontaneous nature of H$_2$ adsorption. The analysis of bonding nature revealed non-covalent interactions between the metal center and the molecular H$_2$. The H-H distance in the metal-decorated systems indicated that the H$_2$ were trapped in the metal-decorated systems in molecular form. Though Au(I)-decorated systems show lower gravimetric wt% than Ag(I)- decorated systems, interestingly it is observed that H$_2$-trapped Au(I)- decorated systems are more stable and indicate spontaneity of H$_2$adsorption-desorption process at higher temperature than Ag(I)-decorated systems. We designed and started our project two years back; to investigate the H$_2$ storage capacity of coinage metal (Cu/Ag/Au) decorated AH systems, and we recently reported the efficiency of Cu-decorated systems in the book 'Computational Studies: From Molecules to Materials', CRC Press/Tylor & Francis Group,[64] and very recently, Journal of the American chemical society (JACS) has published the synthetically established air-stable Cu(I) metal-organic framework (MOF) as hydrogen storage material.[43] It inspired
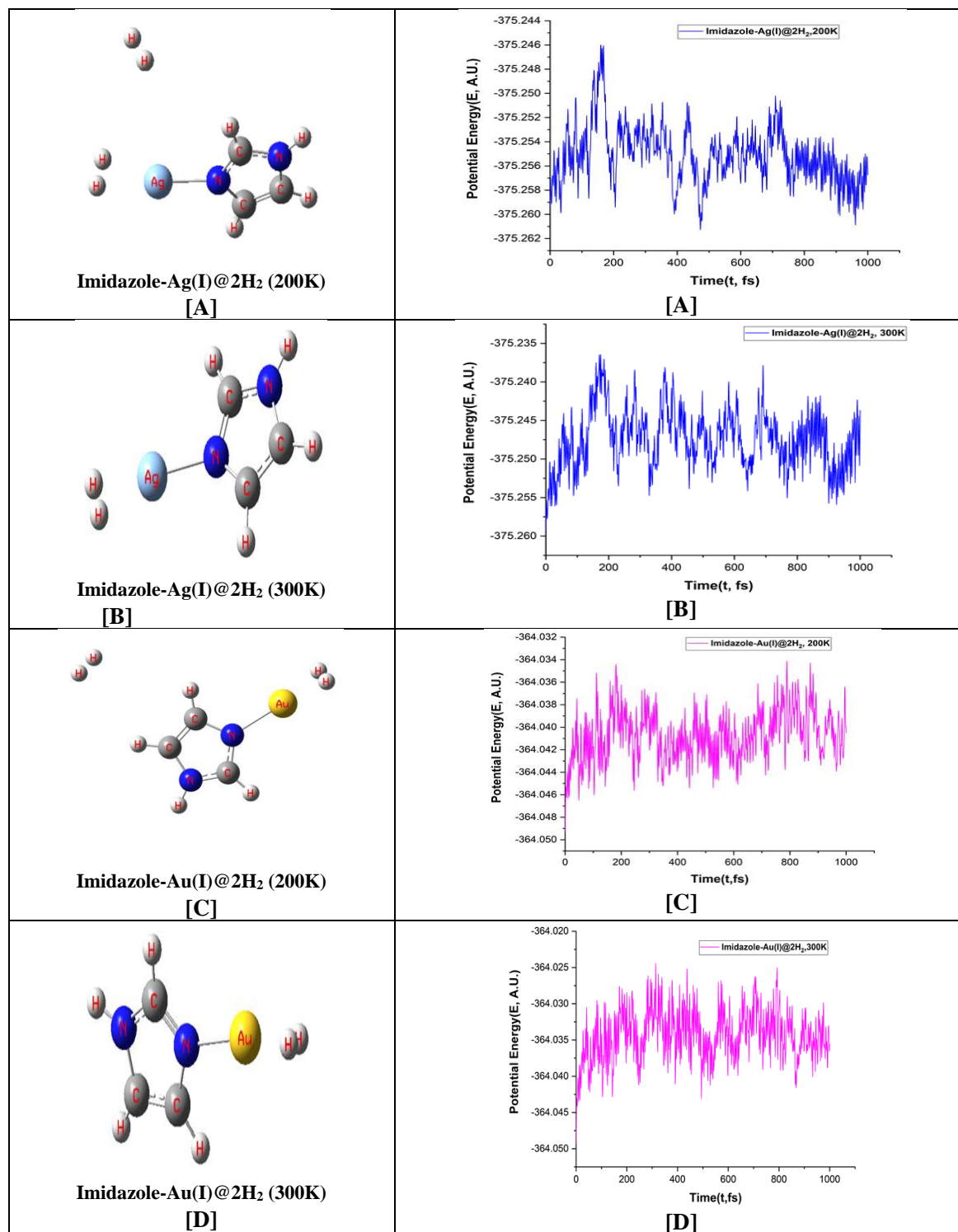
Fig. 11 Simulated structures and Potential Energy (E, A.U.) vs Time (t, fs) of Ag(I)/Au(I) decorated AH system @2H$_2$ (AH = Imidazole) complexes at 300 K and 200 K and at 1000 fs obtained at the wb97xd/sdd level of theory.

us to investigate further the H$_2$ storage capacity of Ag(I)/Au(I)-AH systems, with the believe that our theoretical conclusion will help the synthetic laboratories to establish it in reality. The achieved results (gravimetric wt. %) of all the studied systems meet the target set by the US Department of Energy (2025) for coinage metal systems, and Ag(I)/Au(I)-imidazole and pyrazole systems showed highest gravimetric wt % among others. From the DOS and PDOS values, it can be concluded that all the fragments of the different systems

(aromatic heterocyclic ring, metal ion, and molecular hydrogen respectively) significantly contribute to the formation of the FMOs. The ADMP analysis suggested the complexes can retain H$_2$ molecules at lower temperature up to 1000 fs, and desorption starts when the temperature is increased, and at the room temperature at least one molecular H$_2$ is attached to the systems. From this it can be concluded that both metal decorated Ag(I)/Au(I)-AH model systems survive upon H$_2$ adsorption even at room temperature.

Therefore, these metal-decorated Ag(I)/Au(I)-AH systems are the promising hydrogen storage systems, in designing of efficient storage material.

Acknowledgement

Conflict of Interest

There is no conflict of interest.

Supporting Information

Applicable.

References

[1] L. Schlapbach, A. Züttel, Hydrogen-storage materials for mobile applications, *Nature*, 2001, **414**, 353-358, doi: 10.1038/35104634.

[2] A. Züttel, P. Wenger, P. Sudan, P. Mauron, S.-I. Orimo, Hydrogen density in nanostructured carbon, metals and complex materials, *Materials Science and Engineering: B*, 2004, **108**, 9-18, doi: 10.1016/j.mseb.2003.10.087.

[3] G. Lefevre, S. Saitzek, R. Desfeux, N. Kunkel, A. Sayede, Hydrogen storage in MgX (X = Cu and Ni) systems - is there still news? *Journal of Power Sources*, 2018, **402**, 394-401, doi: 10.1016/j.jpowsour.2018.09.043.

[4] C.-J. Winter, Hydrogen energy Abundant, efficient, clean: a debate over the energy-system-of-change, *International Journal of Hydrogen Energy*, 2009, **34**, S1-S52, doi: 10.1016/j.ijhydene.2009.05.063.

[5] P. Moriarty, D. Honnery, Hydrogen's role in an uncertain energy future, *International Journal of Hydrogen Energy*, 2009, **34**, 31-39, doi: 10.1016/j.ijhydene.2008.10.060.

[6] L. Schlapbach, A. Züttel, Hydrogen-storage materials for mobile applications, *Nature*, 2001, **414**, 353-358, doi: 10.1038/35104634.

[7] Y. H. Hu, Novel hydrogen storage systems and materials, *International Journal of Energy Research*, 2013, **37**, 683-685, doi: 10.1002/er.3056.

[8] W. Luo, P. G. Campbell, L. N. Zakharov, S.-Y. Liu, A single-component liquid-phase hydrogen storage material, *Journal of the American Chemical Society*, 2011, **133**, 19326-19329, doi: 10.1021/ja208834v.

[9] A. Tlahuice-Flores, Hydrogen storage on volleyballene, *Physical Chemistry Chemical Physics*, 2018, **20**, 21251-21256, doi: 10.1039/c8cp01987h.

[10] L.-J. Ma, J. Wang, M. Han, J. Jia, H.-S. Wu, X. Zhang, Linear complex HC C-TMH (TM=Sc–Ni): a simple and efficient adsorbent for hydrogen molecules, *International*

[11] S. Mondal, S. Giri, P. K. Chattaraj, Possibility of having HF-doped hydrogen hydrates, *The Journal of Physical Chemistry C*, 2013, **117**, 11625-11634, doi: 10.1021/jp401342r.

[12] S. S. Ray, S. R. Sahoo, S. Sahu, Hydrogen storage in scandium decorated small boron clusters (BnSc2, n=3-10): a density functional study, *International Journal of Hydrogen Energy*, 2019, 12, 60196030. doi: 10.1016/j.ijhydene.2018.12.109.

[13] T. He, H. Cao, P. Chen, Complex hydrides for energy storage, conversion, and utilization, *Advanced Materials*, 2019, **31**, 1902757, doi: 10.1002/adma.201902757.

[13] T. He, H. Cao, P. Chen, Complex hydrides for energy storage, conversion, and utilization, *Advanced Materials*, 2019, **31**, 1902757, doi: 10.1002/adma.201902757.

[14] T. Sadhasivam, H.-T. Kim, S. Jung, S.-H. Roh, J.-H. Park, H.-Y. Jung, Dimensional effects of nanostructured Mg/MgH2 for hydrogen storage applications: a review, *Renewable and Sustainable Energy Reviews*, 2017, **72**, 523-534, doi: 10.1016/j.rser.2017.01.107.

[15] M.-Q. Fan, S.-S. Liu, Y. Zhang, J. Zhang, L.-X. Sun, F. Xu, Superior hydrogen storage properties of MgH2–10wt.% TiC composite, *Energy*, 2010, **35**, 3417-3421, doi: 10.1016/j.energy.2010.04.034.

[16] E. Kikkinides, M. Georgiadis, A. Stubos, Dynamic modelling and optimization of hydrogen storage in metal hydride beds, *Energy*, 2006, **31**, 2428-2446, doi: 10.1016/j.energy.2005.10.036.

[17] L. Yang, Y. Ma, Y. Xu, G. Chang, Cation–π induced lithium-doped conjugated microporous polymer with remarkable hydrogen storage performance, *Chemical Communications*, 2019, **55**, 11227-11230, doi: 10.1039/c9cc04174e.

[18] R. Pedicini, B. Schiavo, P. Rispoli, A. Saccà, A. Carbone, I. Gatto, E. Passalacqua, Progress in polymeric material for hydrogen storage application in middle conditions, *Energy*, 2014, **64**, 607-614, doi: 10.1016/j.energy.2013.11.073.

[19] P. Chen, Z. Xiong, J. Luo, J. Lin, K. L. Tan, Interaction of hydrogen with metal nitrides and imides, *Nature*, 2002, **420**, 302-304, doi: 10.1038/nature01210.

[20] A. S. Shalabi, H. O. Taha, K. A. Soliman, S. Abeld Aal, Hydrogen storage reactions on titanium decorated carbon nanocones theoretical study, *Journal of Power Sources*, 2014, **271**, 32-41, doi: 10.1016/j.jpowsour.2014.07.158.

[21] Q. Xue, M. Wu, X. C. Zeng, P. Jena, Co-mixing hydrogen and methane may double the energy storage capacity, *Journal of Materials Chemistry A*, 2018, **6**, 8916-8922, doi: 10.1039/c8ta01909f.

[22] A. A. Ensafi, M. Jafari-Asl, A. Nabiyan, B. Rezaei, M. Dinari, Hydrogen storage in hybrid of layered double hydroxides/reduced graphene oxide using spillover mechanism, *Energy*, 2016, **99**, 103-114, doi: 10.1016/j.energy.2016.01.042.

[23] G. K. Dimitrakakis, E. Tylianakis, G. E. Froudakis, Pillared graphene: a new 3-D network nanostructure for enhanced hydrogen storage, *Nano Letters*, 2008, **8**, 3166-3170, doi: 10.1021/nl801417w.

[24] J. L. C. Rowsell, O. M. Yaghi, Effects of functionalization, catenation, and variation of the metal oxide and organic linking units on the low-pressure hydrogen adsorption properties of metal–organic frameworks, *Journal of the American Chemical Society*, 2006, **128**, 1304-1315, doi: 10.1021/ja056639q.

[25] Y. Li, R. T. Yang, Significantly enhanced hydrogen storage in metal–organic frameworks via spillover, *Journal of the American Chemical Society*, 2006, **128**, 726-727, doi: 10.1021/ja056831s.

[26] R. K. Sahoo, S. Sahu, Reversible hydrogen storage capacity of Li and Sc doped novel C_8N_8 cage: insights from density functional theory, *International Journal of Energy Research*, 2022, **46**, 22585-22600, doi: 10.1002/er.8562.

[27] Y. Han, Y. Meng, H. Zhu, Z. Jiang, Y. Lei, B. Suo, Y. Lin, Z. Wen, First-principles predictions of potential hydrogen storage materials: novel sandwich-type ethylene dimetallocene complexes, *International Journal of Hydrogen Energy*, 2014, **39**, 20017-20023, doi: 10.1016/j.ijhydene.2014.09.172.

[28] H. Valencia, A. Gil, G. Frapper, Trends in the hydrogen activation and storage by adsorbed 3d transition metal atoms onto graphene and nanotube surfaces: a DFT study and molecular orbital analysis, *The Journal of Physical Chemistry C*, 2015, **119**, 5506-5522, doi: 10.1021/jp512920f.

[29] S. R. Naqvi, T. Hussain, W. Luo, R. Ahuja, Metallized siligraphene nanosheets (SiC7) as high capacity hydrogen storage materials, *Nano Research*, 2018, **11**, 3802-3813, doi: 10.1007/s12274-017-1954-z.

[30] S. Dong, E. Lv, J. Wang, C. Li, K. Ma, Z. Gao, W. Yang, Z. Ding, C. Wu, I. D. Gates, Construction of transition metal-decorated boron doped twin-graphene for hydrogen storage: a theoretical prediction, *Fuel*, 2021, **304**, 121351, doi: 10.1016/j.fuel.2021.121351.

[31] A. Bhattacharya, S. Bhattacharya, C. Majumder, G. P. Das, Transition-metal decoration enhanced room-temperature hydrogen storage in a defect-modulated graphene sheet, *The Journal of Physical Chemistry C*, 2010, **114**, 10297-10301, doi: 10.1021/jp100230c.

[32] A. N. Sosa, F. de Santiago, Á. Miranda, A. Trejo, F. Salazar, L. A. Pérez, M. Cruz-Irisson, Alkali and transition metal atom-functionalized germanene for hydrogen storage: a DFT investigation, *International Journal of Hydrogen Energy*, 2021, **46**, 20245-20256, doi: 10.1016/j.ijhydene.2020.04.129.

[33] P. Panigrahi, A. Kumar, A. Karton, R. Ahuja, T. Hussain, Remarkable improvement in hydrogen storage capacities of two-dimensional carbon nitride (g-C_3N_4) nanosheets under selected transition metal doping, *International Journal of Hydrogen Energy*, 2020, **45**, 3035-3045, doi: 10.1016/j.ijhydene.2019.11.184.

[34] H. He, X. Chen, W. Zou, R. Li, Transition metal decorated covalent triazine-based frameworks as a capacity hydrogen storage medium, *International Journal of Hydrogen Energy*, 2018, **43**, 2823-2830, doi: 10.1016/j.ijhydene.2017.12.068.

[35] M. K. Dash, S. Das, S. Giri, G. Chandra De, G. Roymahapatra, Comprehensive in silico study on lithiated Triazine isomers and its H_2 storage efficiency, *Journal of the Indian Chemical Society*, 2021, **98**, 100134, doi: 10.1016/j.jics.2021.100134.

[36] M. K. Dash, G. Roymahapatra, S. D. Chowdhury, R. Chatterjee, S. P. Maity, M. Huang, M. N. Bandyopadhyay and Z. Guo, Computational investigation on lithium fluoride for efficient hydrogen storage system, *Engineered Science*, 2022, **18**, 98-104, doi: 10.30919/es8d658.

[37] M. Kanti Dash, S. Sinha, H. Sekhar Das, G. Chandra De, S. Giri, G. Roymahapatra, H_2 storage capacity of Li-doped five-member aromatic heterocyclic superalkali complexes; an in silico study, *Sustainable Energy Technologies and Assessments*, 2022, **52**, 102235, doi: 10.1016/j.seta.2022.102235.

[38] R. Parida, M. K. Dash, S. Giri, G. Roymahapatra, Aromatic N-Heterocyclic superalkali $M@C_4H_4N2$ complexes (M=Li, Na, K); A promising potential hydrogen storage system, *Journal of the Indian Chemical Society*, 2021, **98**, 100065, doi: 10.1016/j.jics.2021.100065.

[39] M. K. Dash, S. Das, S. Giri, G. Chandra De, G. Roymahapatra, Comprehensive in silico study on lithiated Triazine isomers and its H_2 storage efficiency, *Journal of the Indian Chemical Society*, 2021, **98**, 100134, doi: 10.1016/j.jics.2021.100134.

[40] G. Roymahapatra, M. K. Dash, S. Sinha, G. C. De, Z. Guo, Theoretical investigation of hydrogen adsorption efficiency of[oxadiazole- xLi+]complexes (x = 1, 2): in pursuit of green fuel storage, *Engineered Science*, 2022, **19**, 114-124, doi: 10.30919/es8d671.

[41] G. Roymahapatra, M. K. Dash, A. Ghosh, A. Bag, S. Mishra, S. Maity, Hydrogen storage on Lithium chloride/Lithium bromide surface at cryogenic temperature, *ES Energy & Environment*, 2022, doi: 10.30919/esee8c756.

[42] Q. Sun, Q. Wang, P. Jena, Y. Kawazoe, Clustering of Ti on a C_{60} surface and its effect on hydrogen storage, *Journal of the American Chemical Society*, 2005, **127**, 14582-14583, doi: 10.1021/ja0550125.

[43] D. Sengupta, P. Melix, S. Bose, J. Duncan, X. Wang, M. R. Mian, K. O. Kirlikovali, F. Joodaki, T. Islamoglu, T. Yildirim, R. Q. Snurr, O. K. Farha, Air-stable Cu(I) metal–organic framework for hydrogen storage, *Journal of the American Chemical Society*, 2023, **145**, 20492-20502, doi: 10.1021/jacs.3c06393.

[44] Gaussian 16, Revision A.03, Wallingford CT: Gaussian, Inc., 2016. https://gaussian.com.

[45] R. G. Parr, W. Yang, Density-functional Theory of Atoms and Molecules, New York: Oxford University Press; (Chapter 2), 1989, 05-15, doi:10.1007/978-94-009-9027-2_2.

[46] K. D. Sen, C. K. Jorgensen, Electronegativity; Structure and Bonding, 66. *Berlin: Springer*, 1987, doi: 10.1002/bbpc.19890930424.

[47] R. G. Parr, L. V. Szentpály, S. Liu, Electrophilicity index, *Journal of the American Chemical Society*, 1999, **121**, 1922-1924, doi: 10.1021/ja983494x.

[48] P. K. Chattaraj, Chemical reactivity theory: a density functional view, Boca Raton, FL: *Taylor and Francis, CRC Press*; 2009, doi: 10.1201/9781420065442

[49] Z. Chen, C. S. Wannere, C. Corminboeuf, R. Puchta, P. von Ragué Schleyer, Nucleus-independent chemical shifts (NICS) as an aromaticity criterion, *Chemical Reviews*, 2005, **105**, 3842-3888, doi: 10.1021/cr030088+.

[50] A. Stanger, NICS–past and present, *European Journal of Organic Chemistry*, 2020, **2020**, 3120-3127, doi: 10.1002/ejoc.201901829.

[51] R. Parida, S. Das, L. J. Karas, J. I.-C. Wu, G. Roymahapatra, S. Giri, Superalkali ligands as a building block for aromatic trinuclear Cu(i)–NHC complexes, *Inorganic Chemistry Frontiers*, 2019, **6**, 3336-3344, doi: 10.1039/c9qi00873j.

[52] T. Lu, F. Chen, Multiwfn: A multifunctional wavefunction analyzer, *Journal of Computational Chemistry*, 2012, **33**, 580-592, doi: 10.1002/jcc.22885.

[53] A. Ebrahimi, M. Izadyar, M. Khavani, Theoretical design of a new hydrogen storage based on the decorated phosphorene nanosheet by alkali metals, *Journal of Physics and Chemistry of Solids*, 2023, **178**, 111354, doi: 10.1016/j.jpcs.2023.111354.

[54] H. O. Edet, H. Louis, I. Benjamin, M. Gideon, T. O. Unimuke, S. A. Adalikwu, A. D. Nwagu, A. S. Adeyinka, Hydrogen storage capacity of C12X12 (X=N, P, and Si), *Chemical Physics Impact*, 2022, **5**, 100107, doi: 10.1016/j.chphi.2022.100107.

[55] R. F. W. Bader, P. J. MacDougall, C. D. H. Lau, Bonded and nonbonded charge concentrations and their relation to molecular geometry and reactivity, *Journal of the American Chemical Society*, 1984, **106**, 1594-1605, doi: 10.1021/ja00318a009.

[56] H. B. Schlegel, J. M. Millam, S. S. Iyengar, G. A. Voth, A. D. Daniels, G. E. Scuseria, M. J. Frisch, *Ab initio* molecular dynamics: Propagating the density matrix with Gaussian orbitals, *The Journal of Chemical Physics*, 2001, **114**, 9758-9763, doi: 10.1063/1.1372182.

[57] S. S. Iyengar, H. B. Schlegel, J. M. Millam, G. A. Voth, G. E. Scuseria, M. J. Frisch, *Ab initio* molecular dynamics: Propagating the density matrix with Gaussian orbitals. II. Generalizations based on mass-weighting, idempotency, energy conservation and choice of initial conditions, *The Journal of Chemical Physics*, 2001, **115**, 10291-10302, doi: 10.1063/1.1416876.

[58] R. Parida, M. Rath, S. Sinha, G. Roymahapatra, S. Giri, Organic and inorganic benzene transform to superalkalis: An in silico study, *Journal of Indian Chemical Society*, 2020, **97**, 2689-2697.

[59] R. G. Pearson, The principle of maximum hardness, *Accounts of Chemical Research*, 1993, **26**, 250-255, doi: 10.1021/ar00029a004.

[60] E. Chamorro, P. K. Chattaraj, P. Fuentealba, Variation of the electrophilicity index along the reaction path, *The Journal of Physical Chemistry A*, 2003, **107**, 7068-7072, doi: 10.1021/jp035435y.

[61] C. Guo, C. Wang, The theoretical research of hydrogen storage capacities of Cu3Bx (X=1–4) compounds under ambient conditions, *International Journal of Hydrogen Energy*, 2020, **45**, 24947-24957, doi: 10.1016/j.ijhydene.2020.06.089.

[62] R. Parida, G. N. Reddy, A. Ganguly, G. Roymahapatra, A. Chakraborty, S. Giri, On the making of aromatic organometallic superalkali complexes, *Chemical Communications*, 2018, **54**, 3903-3906, doi: 10.1039/c8cc01170b.

[63] R. Parida, M. Rath, S. Sinha, G. Roymahapatra and S. Giri, Organic and inorganic benzene transform to superalkalis: An in silico study, *Journal of Indian Chemical Society*, 2020, **97**, 2689-2697. doi-: 10.5281/zenodo.5656084

[64] A. Bag, M. K. Dash, S. Giri, G. C. De, G. Roymahapatra, Hydrogen Storage Efficiency of Isomeric Cu(I)-Triazine Complexes: In Quest of New Hydrogen Storage Material, Computational Studies: From Molecules to Materials, CRC Press/Tylor & Francis Group, 2023 (In-press).